XLVI CILAMCE
VITÓRIA - ES - BRAZIL - 2025
XLVI IBERO-LATIN AMERICAN CONGRESS ON COMPUTATIONAL METHODS IN ENGENEERING

# On the detection of breast tumors using dynamic thermography and Self-adaptive Differential Evolution

Jan P.A.S. Rocha[1], Felipe S. Loureiro[2], Heder S. Bernardino[1], Helio J.C. Barbosa[1,3]

[1]*Program in Computational Modeling, Federal University of Juiz de Fora*
*Juiz de Fora, 36036-900, Minas Gerais, Brazil*
*jan.rocha@estudante.ufjf.br, heder.bernardino@ufjf.br*
[2]*Department of Thermal and Fluid Sciences, Federal University of São João del-Rei*
*São João del-Rei, 36307-352, Minas Gerais, Brazil*
*felipe.loureiro@ufsj.edu.br*
[3]*National Laboratory for Scientific Computing*
*Petrópolis, 25651-075, Rio de Janeiro, Brazil*
*hcbm@lncc.br*

**Abstract.** Recently, the clinical diagnosis of breast tumors using thermal analysis has gained increasing attention as a non-invasive and cost-effective alternative to traditional techniques. To enhance breast cancer detection and reduce false positive and false negative rates, several authors have suggested the use of dynamic infrared thermography. In this study, we propose a dynamic thermography approach for the detection of breast cancer with tumor focus. We model a circular tumor embedded within a multilayered breast structure composed of five distinct tissue layers. Based on simulated skin surface temperature measurements, the geometric parameters of the tumors are estimated using metaheuristic optimization techniques. To simulate the effects of real-world measurement conditions, random noise is added to the synthetic temperature data, where the noise is consistent with the magnitude typically observed in modern infrared cameras. The forward problem is modeled using a two-dimensional transient bioheat transfer model governed by Pennes' equation, and it is efficiently solved via the Finite Element Method implemented with FEniCS. The inverse problem is formulated as an optimization task and tackled using Self adaptive Differential Evolution, an auto-adaptive variant of Differential Evolution. Numerical experiments, conducted both with and without noise, demonstrate that the proposed approach is a promising alternative for solving inverse problems in breast tumor detection through thermographic analysis.

**Keywords:** Inverse Geometric Problem, Metaheuristics, Pennes' Bioheat Equation, Finite Element Method

## 1 Introduction

Breast cancer, with approximately 2.3 million new cases and 670,000 deaths reported in 2022 [1], remains the most prevalent cancer among women worldwide. Traditionally, its diagnosis relies on imaging techniques such as mammography, ultrasound, and MRI. In recent years, thermography has emerged as a promising complementary tool due to its non-invasive nature and lower operational costs [2, 3], although its clinical use in Brazil remains limited to research purposes [4].

Thermographic approaches generally involve solving an inverse problem that aims to estimate internal tumor characteristics from surface temperature data [2, 5, 6]. Among these, dynamic thermography —which analyzes transient thermal responses following external thermal stimulation—has gained attention for its potential to provide richer information compared to steady-state models [6]. A comparative numerical study of steady-state and transient (dynamic) thermography for breast tumour depth detection can be found at [7]. In this study, we used a transient as well as a steady-state bioheat model for breast cancer based on the Pennes equation [6], and apply it to estimate tumor geometry from synthetic surface temperature data. The inverse problem is solved using a Self-adaptive Differential Evolution strategy, as proposed by Rocha et al. [2], which has shown promising results in similar inverse problems involving metaheuristics such as genetic algorithms and differential evolution [2, 8].

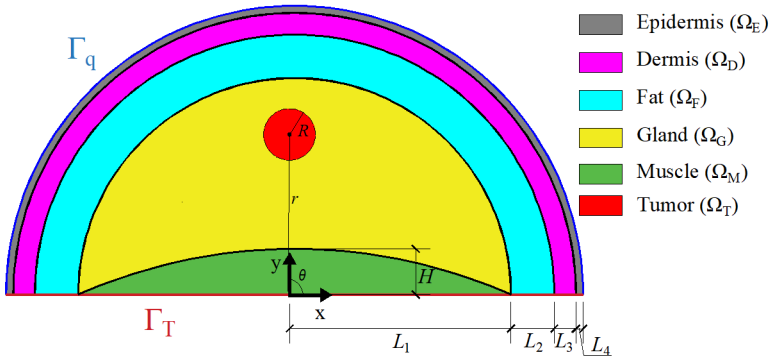



Figure 1. Computational geometric model of the breast, with embedded tumor and boundary labels.

## 2 Inverse Problem Formulation

The proposed inverse problem aims to estimate geometric parameters, such as the center and radius of a tumor. More specifically, after the synthetic (i.e., simulated) acquisition of temperature on the breast surface, an inverse analysis is performed by minimizing the following objective function [6]:

$$F(\mathbf{v}) = \sum_{t=1}^{n_t} \sum_{p=1}^{n_p} \left(T_{p,t}^{e}(\mathbf{v}) - T_{p,t}^{m}\right)^2 \tag{1}$$

where $\mathbf{v}$ is the design variable vector (parameters to be estimated), $F(\mathbf{v})$ is the objective function value, $T^e$ and $T^m$ represent, respectively, the estimated and measured temperatures on the skin surface during the thermal recovery phase, $t$ is the time in which the temperature is measured at point $p$, $n_t$ is the number of observed time instants, and $n_p$ is the number of measurement points. For the steady-state case, $n_t = 1$.

In this work, a simplified two-dimensional geometric model is adopted to represent the breast. Thus, the breast is modeled as a semicircle composed of distinct tissue layers: epidermis, dermis, fat, mammary gland, and muscle (Fig. 1). The thickness of each layer is: i) Epidermis: $0.1$ mm; ii) Dermis: $1.6$ mm; iii) Fat: $5.3$ mm; iv) Gland: $65$ mm; and v) Muscle: at $x = 0$, the height is $H = 15$ mm, with a radius of $65$ mm. Due to the geometric characteristics of the model, polar coordinates are adopted, and the design variables (the center of the tumor and its radius), are defined by the vector $\mathbf{v} = [\theta, r, R]$.

As the tumor search is restricted to the glandular layer, the inverse problem of estimating the unknown geometric parameters contained in $\mathbf{v} \in \mathbb{R}^3$ can be reformulated as a constrained minimization problem:

$$\begin{aligned}
&\min_{\mathbf{v}} F(\mathbf{v}); \quad \mathbf{v} = [\theta, r, R] \\
&\text{subject to:} \\
&g^{(1)}(\mathbf{v}) = \sqrt{(x_M - r\cos\theta)^2 + (y_M - r\sin\theta)^2} - (R_M + R) \geq 0; \\
&g^{(2)}(\mathbf{v}) = L_1 - R - r \geq 0; \\
&0 < \theta < \pi; \quad 0 < r < L_1; \quad R^{(L)} < R < R^{(U)}.
\end{aligned} \tag{2}$$

The search space is limited by $R^{(L)} = 1$ mm (lower bound) and $R^{(U)} = 10$ mm (upper bound). The muscle is represented by an arc with center at $x_M = 0$ and $y_M = H - R_M$, with a radius $R_M = (H^2 + L_1^2)/(2H)$. The constraint $g^{(1)}(\mathbf{v})$ prevents tumors from invading the muscle layer, while $g^{(2)}(\mathbf{v})$ prevents intersection with the fat layer. Individuals who do not satisfy $g^{(1)}(\mathbf{v})$ or $g^{(2)}(\mathbf{v})$ are classified as infeasible; otherwise, they are feasible.

## 3 Inverse Problem via SaDE

The proposed methodology involves the search for geometric parameters by minimizing the least squares norm of the difference between the estimated and measured temperatures throughout the entire observation period

after applying the thermal stress until thermal stabilization in the transient case, and the estimated temperature in the steady-state case. The use of Differential Evolution (DE) and Self-Adaptive Differential Evolution (SaDE) was proposed by Rocha et al. [2] to solve the optimization problem in the static case. The results obtained were compared to those reached by a Genetic Algorithm, that is widely used in the literature, and SaDE showed superior performance and has less user-defined parameters.

SaDE is a DE variant with self-adaptation of its parameters [9]. After the learning period ($LP$), the parameters $CR$ and $F$ are updated for each DE variant ($k$) (mutation strategies), based on the average of previously successful values. Then, the probability $p_k$ of selecting each search strategy is adjusted according to the success rate of each of the six considered strategies [9, 10]: i) DE/rand/1; ii) DE/best/1; iii) DE/rand/2; iv) DE/best/2; v) DE/current-to-best/1; and vi) DE/current-to-best/1. The pseudocode of SaDE is presented in Algorithm 1.

**Algorithm 1** Self-adaptive Differential Evolution

```
pop ← Generate random population
while stop criterion not satisfied do
    for i = 0 to Size(pop) do
        if G < LP then
            ParameterAdaptation(CR, F)
        end if
        v*_i ← SelectFunction(p_k, F, pop)                ▷ Mutation
        j ←U(0, Size(v_i))
        for k <Size(v_i) do                               ▷ Crossover
            if U(0, 1) < CR and j ≠ k then
                v*_{i,k} ← v_{i,k}
            end if
        end for
        if F(v*_i) < F(v_i) then                          ▷ Selection
            v_i ← v*_i
        end if
    end for
end while
```

## 4 Forward Problem via FEM using FEniCS

The use of mathematical models for the simulation of the temperature distribution inside the breast is a fundamental step in tumor detection using the proposed method. For a more realistic representation, the model used should account for three main factors [11]: (i) blood perfusion, (ii) vascular architecture, and (iii) variations in thermal properties and blood flow rate.

The Pennes model, although simplifying the bioheat transfer problem, is widely used in the context of this application [12]. This model is also applied in other fields such as hyperthermia therapy, blood perfusion measurements, cryosurgery, and whole-body simulations, showing theoretical results that are consistent with experimental data [11]. The Pennes' bioheat equation is given by:

$$\nabla \cdot (k\nabla T) + \omega_b \rho_b c_b (T_a - T) + Q_m = \rho c_p \frac{\partial T}{\partial t}, \quad \text{in} \bigcup_{i=E,D,F,G,M,T} \Omega_i. \tag{3}$$

where $\rho_b = 1060$ kg/m$^3$, $c_b = 3770$ J/(kg °C), $T_a = 37$ °C, and $\omega_b$ represent the blood density, specific heat of the blood, arterial temperature, and blood perfusion rate, respectively. For the tissue, $T$, $k$, $Q_m$, $c_p$ and $\rho$ correspond to the temperature field, thermal conductivity, metabolic heat generation, specific heat and effective density respectively.

The boundary conditions are given by:

$$\begin{aligned} &T = 37^0 C, && \text{on } \Gamma_T \\ &\begin{cases} T = T_{stress},\ t \le t_{stress} \\ -k\nabla T \cdot \mathbf{n} = h_c \left(T - T_\infty\right),\ t > t_{stress} \end{cases}, && \text{on } \Gamma_q \end{aligned} \tag{4}$$

where $h_c$ is the convective heat transfer coefficient, and $T_\infty$ is the ambient temperature. The stationary solution therefore serves as the initial condition for the transient case.

As no analytical solution is available, the problem is solved numerically using the Finite Element Method (FEM) implemented in the open-source FEniCS library. A mesh sensitivity analysis by computing the difference of the temperatures on the skin surface and considering a fine mesh as the reference solution was carried out to balance accuracy and computational cost. The analysis showed that meshes with about $1.5 \times 10^4$ nodes provide reliable accuracy, since further refinement yields differences below the 30 mK resolution of thermographic cameras. Therefore, `cellSize` = 35 (FEniCS parameter) was chosen, producing meshes with local refinements around tumor regions and $N = 67$ fixed surface points. The time derivative is approximated using a finite difference scheme based on the implicit Euler method. All numerical implementations, including mesh generation, boundary condition handling, and time-stepping procedures, are carried out within the FEniCS framework. Further implementation details for the steady-state case can be found in Rocha et al. [2]

## 5 Results and Discussion

Based on the literature [13–16], the thermophysical properties of tissues and the metabolic heat generation values used for all layers and the tumor are presented in Table 1. During the stress phase, a time step of $\Delta t = 20$ s was used; during the recovery phase, $\Delta t = 200$ s was applied, and the final observation time was set to 3600 s. The stress temperature was $T_{stress} = 4$°C for a duration of $t_{stress} = 60\ s$ [6, 7]. For boundary conditions we set $h_c = 10W/m^{2\circ}C$ (natural convection) and $T_\infty = 25$°C.

Table 1. Thermophysical properties and metabolic heat generation for tissue layers

| Tissue Layer | Thermal conductivity $k$ [W/(m °C)] | Blood perfusion rate $\omega_b \times 10^{-4}$ [m$^3$/s/m$^3$] | Metabolic heat generation $Q_m$ [W/m$^3$] | Specific heat $c_p$ [J/kgK] | Effective density $\rho$ [kg/m$^3$] |
|---|---|---|---|---|---|
| Epidermis | 0.235 | 0 | 0 | 3589 | 1200 |
| Dermis | 0.445 | 1.8 | 368.1 | 3300 | 1200 |
| Fat | 0.21 | 2.2 | 400 | 2674 | 1000 |
| Gland | 0.48 | 5.4 | 700 | 3770 | 1050 |
| Muscle | 0.48 | 27 | 700 | 3800 | 1085 |
| Tumor | 0.62 | 160 | 50200 | 3770 | 1050 |

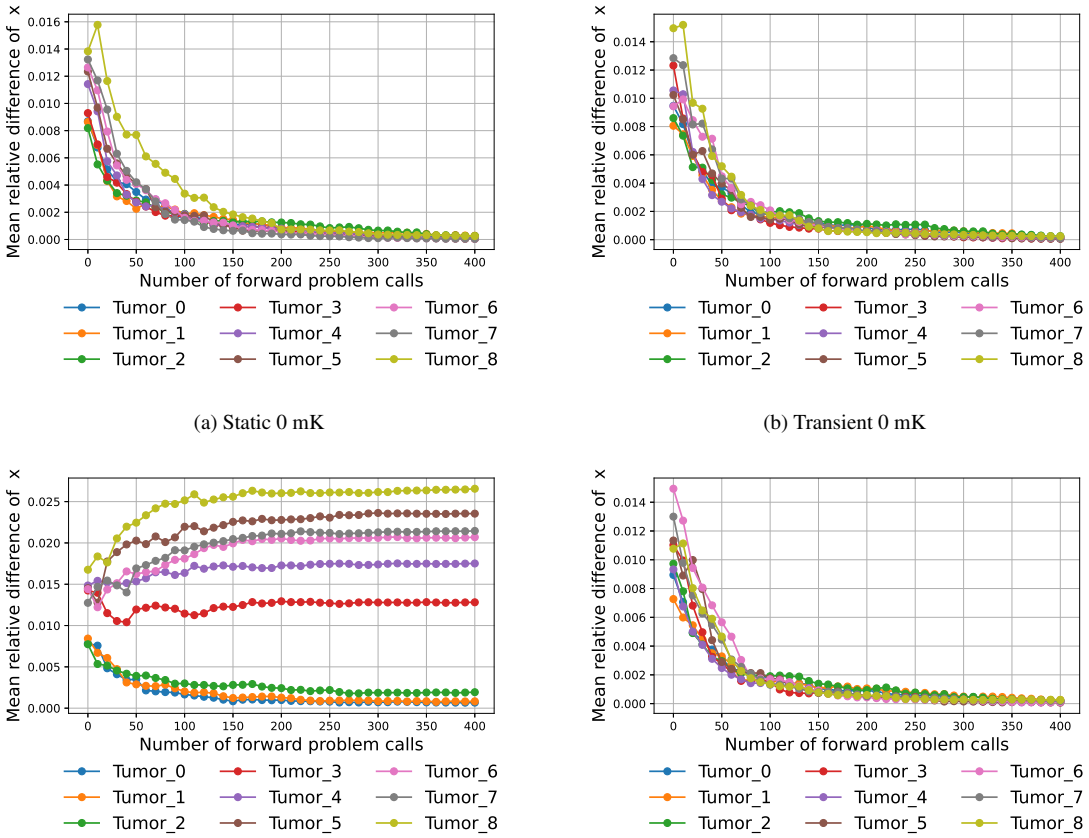
To compare static (steady-state) and dynamic (transient) thermographic exams, nine different synthetic references were proposed, divided into three groups: i) close to the surface; ii) approximately at the midpoint of the breast; and iii) deep inside the breast. The tumors and their respective positions are presented in Table 2. Although polar coordinates were used during the optimization process, the results are presented in Cartesian coordinates to provide a clearer and more intuitive visualization of the data. It is important to note that all tumors were placed at the breast center at $x = 0$.

Table 2. Reference tumor positions

| $y$ | $R$ | Name | $y$ | $R$ | Name | $y$ | $R$ | Name |
|---|---|---|---|---|---|---|---|---|
| 0.058489 | 2.0e-3 | Tumor_0 | 0.0325 | 2.0e-3 | Tumor_3 | 0.02149 | 2.0e-3 | Tumor_6 |
| 0.058489 | 1.5e-3 | Tumor_1 | 0.0325 | 1.5e-3 | Tumor_4 | 0.02149 | 1.5e-3 | Tumor_7 |
| 0.058489 | 1.0e-3 | Tumor_2 | 0.0325 | 1.0e-3 | Tumor_5 | 0.02149 | 1.0e-3 | Tumor_8 |

The reference temperature data on the breast skin surface, i.e., $T^m_{p,t}(\mathbf{v}_{ref})$, were simulated by solving the forward problem, considering the parameters $\mathbf{v}_{ref}$ shown in Table 2. It is assumed that the simulated measurements positions are equally distributed along the boundary $\Gamma_q$ (see Fig. 1), totaling $N = 67$ measurement points. Additionally, to evaluate the search efficiency under more realistic conditions, noise was added to the reference temperature data to simulate uncertainties inherent to experimental measurements [6] as $T^*_{p,t}(\mathbf{v}_{ref}) = T^m_{p,t}(\mathbf{v}_{ref}) + \xi\Delta\hat{T}_u,\ \ p = 1, \ldots, N,\ \ t = 1, \ldots, n_t$, where $\xi \in [-1, 1]$ is a uniformly distributed random number, $\Delta\hat{T}_u$ represents the uncertainty level, and $T^*_k(\mathbf{v}_{ref})$ are the new reference temperatures, now with added noise. According to Iljaž et al. [6], with modern infrared cameras it is possible to achieve a NETD (Noise Equivalent Temperature Difference) below 30 mK; thus, noise levels of 0 mK (no noise) and 50 mK were used [6].

Since this is a evolutionary algorithm, 30 independent runs were performed for each reference to allow statistical analysis. For the inverse problem setup, a population size of 20 individuals was used, with a stopping criterion of 400 forward problem evaluations and a learning period $LP$ of 15 generations. For the steady-state model, the average execution time per run was approximately 2.06 minutes, while for the transient model it was around 25.18 minutes. The results showing the relative difference between the best individual and the reference, are presented in Figs. 2 to 4.




(a) Static 0 mK

(b) Transient 0 mK

(c) Static 50 mK

(d) Transient 50

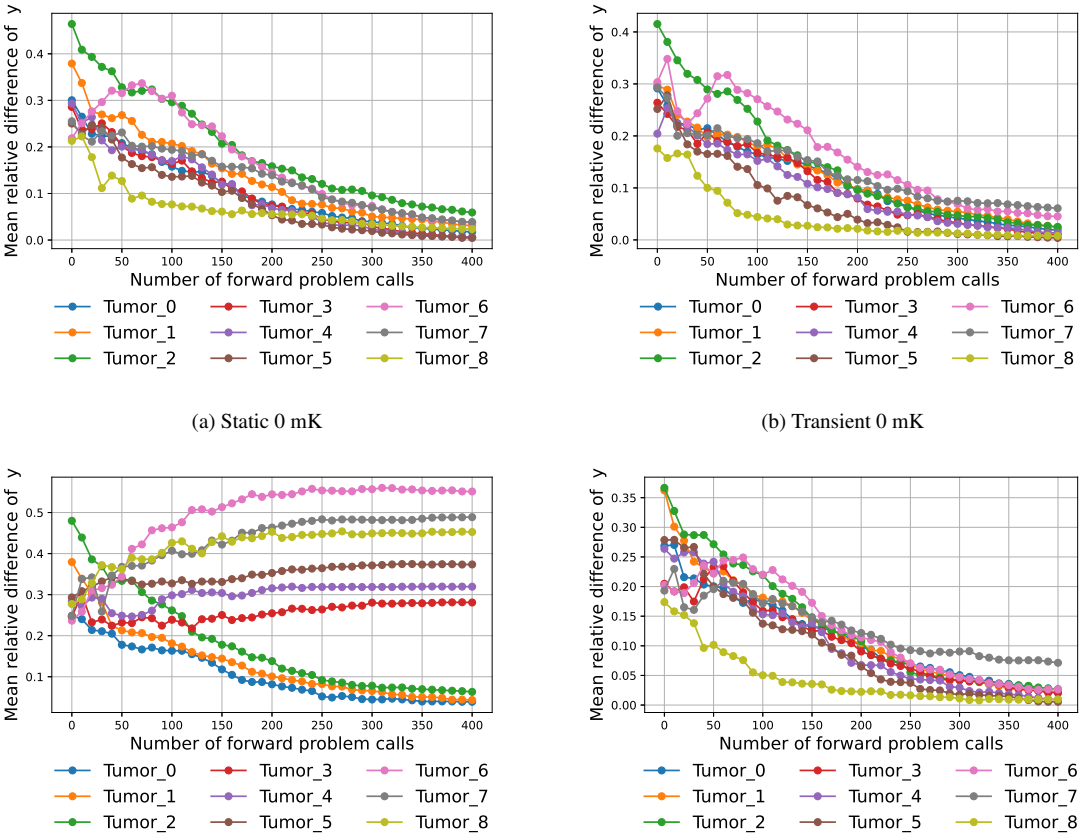
Figure 2. Average relative difference of variable $x$ over generations.

By observing the convergence of the variables, it can be seen that for Tumors 3 to 8, the steady-state algorithm diverges from the actual position when surface temperature noise is present, indicating that the added noise level compromised detection, as its magnitude is on the same order as the temperature difference between healthy tissue and tumor.

The stagnation of the objective function and deviation from the true solution are not observed in the transient case, as the larger number of surface measurements helps mitigate the added noise. This better convergence demonstrates that, despite its higher computational cost, the transient model is a more robust alternative to overcome measurement errors.

## 6 Conclusions

This work presented a methodology for detecting breast tumors using dynamic thermography and Self-adaptive Differential Evolution (SaDE), employing synthetic data and numerical simulations. The results demonstrated that transient thermographic analysis, when compared to the steady-state approach, is more robust to noise, particularly in deeper tumor locations, thereby improving detection reliability. Despite higher computational costs, the transient model yielded better convergence and reduced sensitivity to surface temperature uncertainties, which are inherent in real-world scenarios. The use of SaDE also proved effective, offering consistent estimations with reduced user-defined parameters, making it a promising tool for solving inverse bioheat transfer problems in oncological applications. Future work may explore the incorporation of more realistic breast geometries and validation using clinical or phantom data.




(a) Static 0 mK

(b) Transient 0 mK

(c) Static 50 mK

(d) Transient 50 mK

Figure 3. Average relative difference of variable $y$ over generations.

**Acknowledgments.** We thank the financial support provided by CNPq, CAPES, FAPEMIG, UFSJ/PPMEC/DCTEF, and UFJF.

**Authorship statement.** The authors hereby confirm that they are the sole liable persons responsible for the authorship of this work, and that all material that has been herein included as part of the present paper is either the property (and authorship) of the authors, or has the permission of the owners to be included here.

## References

[1] J. Kim, A. Harper, V. McCormack, H. Sung, N. Houssami, E. Morgan, M. Mutebi, G. Garvey, I. Soerjomataram, and M. M. Fidler-Benaoudia. Global patterns and trends in breast cancer incidence and mortality across 185 countries. *Nature Medicine*, vol. 31, n. 4, pp. 1154–1162, 2025.

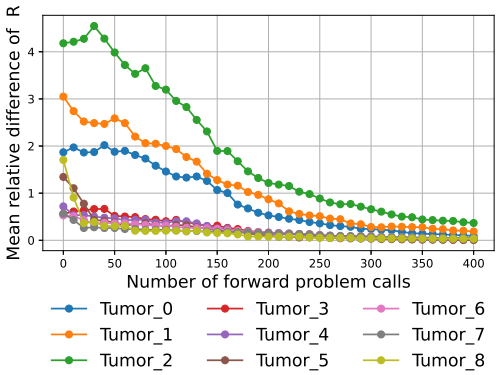
[2] J. P. A. S. Rocha, F. S. Loureiro, H. S. Bernardino, A. B. Vieira, and H. J. C. Barbosa. Metaheuristics applied to the thermographic detection of multicentric breast tumor. *Journal of the Brazilian Society of Mechanical Sciences and Engineering*, vol. 46, n. 6, pp. 361, 2024.

[3] M. Soltani, R. Rahpeima, and F. M. Kashkooli. Breast cancer diagnosis with a microwave thermoacoustic imaging technique — a numerical approach. *Medical & Biological Engineering & Computing*, vol. 57, pp. 1497 – 1513, 2019.

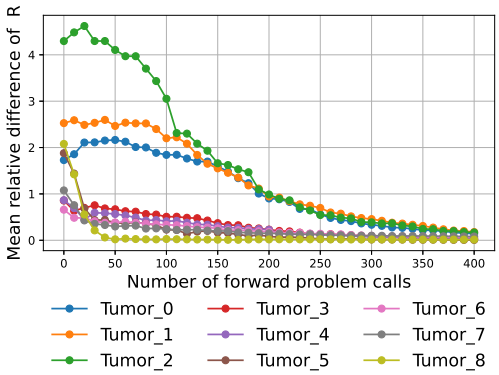
[4] de Câncer José Alencar Gomes da I. N. Silva (INCA). *Diretrizes para a Detecção Precoce do Câncer de Mama no Brasil*. Ministério da Saúde, 2015.

[5] A. A. A. Figueiredo, J. G. do Nascimento, F. C. Malheiros, L. H. da Silva Ignacio, H. C. Fernandes, and G. Guimaraes. Breast tumor localization using skin surface temperatures from a 2D anatomic model without knowledge of the thermophysical properties. *Computer Methods and Programs in Biomedicine*, vol. 172, pp. 65 – 77, 2019.

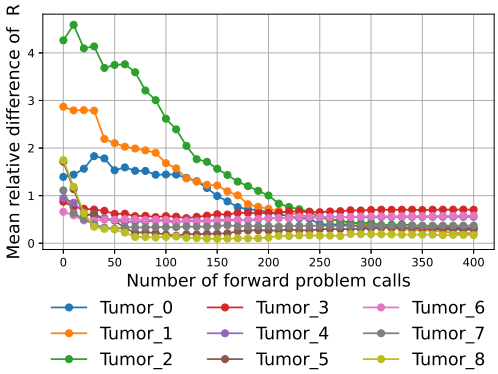
[6] J. Iljaž, L. C. Wrobel, T. Gomboc, M. Hriberšek, and J. Marn. Solving inverse bioheat problems of skin tumour identification by dynamic thermography. *Inverse Problems*, vol. 36, n. 3, pp. 035002, 2020.



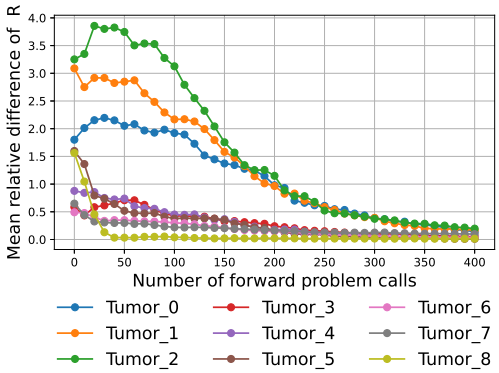

(a) Static 0 mK




(b) Transient 0 mK




(c) Static 50 mK




(d) Transient 50 mK

Figure 4. Average relative difference of variable $R$ over generations.

[7] A. Amri, S. H. Pulko, and A. J. Wilkinson. Potentialities of steady-state and transient thermography in breast tumour depth detection: A numerical study. *Computer Methods and Programs in Biomedicine*, vol. 123, pp. 68–80, 2016.

[8] L. Bezerra, M. Oliveira, T. Rolim, A. Conci, F. Santos, P. Lyra, and R. Lima. Estimation of breast tumor thermal properties using infrared images. *Signal Processing*, vol. 93, n. 10, pp. 2851 – 2863. Signal and Image Processing Techniques for Detection of Breast Diseases, 2013.

[9] A. Banitalebi, M. I. A. Aziz, and Z. A. Aziz. A self-adaptive binary differential evolution algorithm for large scale binary optimization problems. *Information Sciences*, vol. 367-368, pp. 487 – 511, 2016.

[10] A. K. Qin, V. L. Huang, and P. N. Suganthan. Differential evolution algorithm with strategy adaptation for global numerical optimization. *IEEE Trans. on Evolutionary Computation*, vol. 13, n. 2, pp. 398–417, 2009.

[11] L. Jiji. *Heat Conduction*. Springer Berlin Heidelberg, 2009.

[12] J. Y. Murthy, W. J. Minkowycz, E. M. Sparrow, and S. R. Mathur. *Handbook of Numerical Heat Transfer*. John Wiley & Sons, Ltd, 2000.

[13] A. A. Figueiredo, H. C. Fernandes, F. C. Malheiros, and G. Guimaraes. Influence analysis of thermophysical properties on temperature profiles on the breast skin surface. *Intl. Communications in Heat and Mass Transfer*, vol. 111, pp. 104453, 2020.

[14] J. Iljaž, L. C. Wrobel, M. Hriberšek, and J. Marn. Numerical modelling of skin tumour tissue with temperature-dependent properties for dynamic thermography. *Computers in Biology and Medicine*, vol. 112, pp. 103367, 2019.

[15] Y. Zhou and C. Herman. Optimization of skin cooling by computational modeling for early thermographic detection of breast cancer. *Intl. Journal of Heat and Mass Transfer*, vol. 126, pp. 864–876, 2018.

[16] A. Bhattacharya and R. Mahajan. Temperature dependence of thermal conductivity of biological tissues. *Physiological Measurement*, vol. 24, n. 3, pp. 769, 2003.